ZIBELINE INTERNATIONAL™ PUBLISHING

ISSN: 2521-2915 (Print)
ISSN: 2521-2923 (Online)
CODEN: PJGABN

Pakistan Journal of Geology (PJG)

DOI: http://doi.org/10.26480/pjg.01.2024.44.56

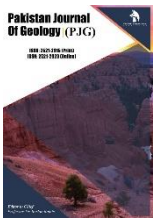

CrossMark

RESEARCH ARTICLE

# GROUNDWATER INVESTIGATION USING ELECTRICAL RESISTIVITY METHOD IN A BASEMENT TERRAIN OF SANNGO ELERE, ERUWA, SOUTHWESTERN NIGERIA

**Adedokun Damilola Rukayat[a*], Ishola K.S.[b], Alli Adnan Karram[a], Ibitomi Michael Adewale[c]**

*[a]Department of Physics, Lead City University, Ibadan, Oyo State, Nigeria*
*[b]Department of Geosciences, University of Lagos, Akoka Lagos*
*[c]Department of Mineral and Petroleum Resources Engineering, Kogi State Polytechnic, Lokoja*



**ARTICLE DETAILS**

***Article History:***

Received 23 June 2024
Revised 09 July 2024
Accepted 19 August 2024
Available online 21 August 2024

**ABSTRACT**

Groundwater Investigation was carried out using Electrical Resistivity Method at Sanngo Elere, Eruwa. There are many hand-dug wells in the study area but there is no evidence that groundwater exploration has been carried out in the area. Vertical Electrical Sounding (VES) was carried out in the area with the aim of determining viable aquiferous zone. Twenty (20) VES were carried out using Schlumberger electrode array configuration. The VES data generated were processed and interpreted using partial curve matching method and computer iterative modelling software called win resist. The interpreted data revealed three to five geoelectric sections consisting of the topsoil with resistivity ranging from 149 to 1407Ωm. Weathered/party weathered layer with resistivity and thickness values ranging from 131 to 2082Ωm and 1.0 to 14.2m respectively. A partly weathered/fresh basement rock with resistivity and thickness values that ranges from 45 to 3297Ωm and 2.6 to 21.6m. also a fresh basement rock with resistivity values that range from 1020 – 8744Ωm. On the bases of the resistivity and thickness of fracture zone, twelve out of 20 VES points are promising location for prolific borehole. The values of computed reflection coefficient were further used to confirm water bearing fractures. Electrical Resistivity Survey has been successfully utilized for groundwater exploration in the study area.

**KEYWORDS**

Groundwater Exploration, aquiferous zone, computer iterative, Electrical Resistivity, Reflection coeffient.

## 1. INTRODUCTION

Access to safe drinking water is a key ingredient for better health and reducing poverty. Groundwater is the water found below the surface of land and it exists in pores between sedimentary particles and fissures of hard rocks (Ilugbo and Adebiyi 2017; Adebiyi et al., 2018; Adebo et al., 2018; Adeboe etal., 2022; Bawallah et al., 2021a; Bawallah et al., 2024; Ozegin et al., 2024a). Groundwater sustains the flow of surface water during dry periods and also groundwater is more preferable due to its less contamination (Bawallah et al., 2021b; Ozegin et al., 2024b). However, geophysical methods have been applied in different geological environments for groundwater exploration (Adebo et al., 2019; Bawallah et al., 2020a; Ilugbo et al., 2023b; Ozegin et al., 2023). Electrical resistivity method has been used in many geophysical investigations, permafrost mapping and geological mapping. The electrical methods are generally classified according to the energy source involved i.e. natural or artificial methods (Jatau eta., 2013; Ilugbo et al., 2018a; Bawallah et al., 2020b). The electrical resistivity technique is an effective tool in delineating areas of good potential for groundwater development (Bawallah et al., 2018a; Bawallah et al., 2018b; Ilugbo et al., 2023a). For example, the goal of Vertical Electrical Sounding (VES) is to observe resistivity variation with depth. The Schlumberger configuration is most commonly used for VES investigation. The use of very low frequency electromagnetic (VLF-EM) and vertical electrical sounding (VES) for groundwater exploration is popular in the basement complex rocks terrains because of the occurrence nature of the aquifer (Palacky et al., 1981; Ilugbo et al., 2018b; Ozegin et al., 2024c). The electrical resistivity method has also been used extensively in groundwater investigation in the basement complex terrains (Barongo and Palacky, 1991; Olayinka and Olorunfemi, 1992; Ayolabi et al., 2004; Abiola et al., 2009; Ilugbo et al., 2018c). Investigation of groundwater in Basement Complex terrain poses a challenge in locating fractured bedrock, requiringa detailed understanding of the nature and characteristics of the basement rock (Ilugbo et al., 2019). However, many boreholes have been drilled into a dry fractured or thin weathered layer with a low yield. This is because proper geophysical surveys have not been carried out before the drilling exercise in the study area. Against this background, this study usedthe electrical resistivity method to know the subsurface conditions under investigation (Ilugbo et al., 2020). Furthermore, because of the occurrence nature of shallow water prone to contamination, groundwater should have been an alternative water source. Still, there is a challenge locating highly productive aquifers in different parts of Eruwa. Investigation of groundwater in basement terrain possess a challenge in locating fractured bedrock and this required detailed understanding of the nature and characteristics of the basement rock. However, many boreholes have been drilling into a dry fractured and or thin weathered layer with a low yield. This is because proper geophysical surveys have not been carried out before the drilling exercise. Against this background, this study was embarked on to use electrical resistivity method to have a knowledge of the subsurface conditions under investigation.

## 2. STUDY AREA

The study area is located at Sanngo, Eleresite, Eruwa which fall within Latitudes 07⁰ 32' 19.35'' N and Longitudes03 25 34.15 E (Figure 1). The study area generally experiences the typical tropical climate of average high temperatures and high relative humidity with a rainfall period from March to October. The mean temperatures are highest at the end of the Harmattan (averaging 28°C), from the middle of January to the onset of the

| Quick Response Code | Access this article online | |
|---|---|---|
| | Website: www.pakjgeology.com | DOI: 10.26480/pjg.01.2024.44.56 |

Cite The Article: Adedokun Damilola Rukayat, Ishola K.S., Alli Adnan Karram, Ibitomi Michael Adewale (2024). Groundwater Investigation Using Electrical Resistivity Method in A Basement Terrain of Sanngo Elere, Eruwa, Southwestern Nigeria. *Pakistan Journal of Geology, 8(1): 44-56.*

rains in the middle of March. During the rainfall season, average temperatures are between 24°C and 25°C, while the annual temperature range is about 6°C. Rainfall varies from an average of 1200 mm at the onset of heavy rains to 1800 mm at its peak. The area investigated is predominantly undulation upland terrain. It is characterised by high-left hills, valleys and plain land. The average height of the hills is approximately meters above sea level. The hills are predominantly massive and littered with boulders. The major trends of the ridges lie in the North-South, North-West – South-East directions. In Eruwa there are rivers and springs in which some prominent rivers and their tributaries flow through the town. The drainage pattern is generally dendritic, where the streams flow over uniform bedrock.The rainforest covers much of Eruwa in Ibarapa Local Government Area. The composition is the large tall, crowned trees mixed with thick undergrowth. The southern parts of the state are covered by the rainforest and derived savannah.


**Figure 1:** Location Map of the Study Area

### 2.1 Geology and Hydrogeology

Geologically, the study area is located within the basement complex terrain of Nigeria. The general geology of Nigeria has been studied by various researchers, (Rahaman, 1988; Oyawoye, 1964, 1972; Cooray, 1972; Dada et al., 1993; Ajibade, 1976). Nigerian rocks can be grouped into crystalline and sedimentary rocks. Half of the crystalline rocks in Nigeria are buried beneath the cretaceous and younger sediments while the other half outcrop largely in the North-central, Southwestern and in three regions from the North to the south along the Cameroon line, that is, Mandara highland, Adamawa Plateau and Oban massif. The crystalline rocks can further be divided into three main groups: Basement Complex, Younger Granite and Tertiary-Recent Volcanics. The evolution of the basement complex is associated with the general evolution of the African continent. The complex comprises gneisses and migmatite with supra-crustal relicts, which have yielded Archean between (C. 2700 Ma) and Proterozoic (C. 2000 Ma) (Dada et al., 1993). Hydrogeologically, the area is made of weathered regolith and fractured/fresh basements.

## 3. METHODOLOGY

### 3.1 Field acquisition of resistivity data

Twenty (20) VES were acquired along five (5) traverses using the Schlumberger electrode array configuration, whereby four (4) VES were conducted on each traverse line (Figure 12). The VES techniques was employed by maintaining the current and potential electrodes at the same relative spacing and the whole spread expanded progressively along a profile. Successive apparent resistivity values were determined at the same center point for increasing values of electrode spacing. The basis for making an electrical sounding irrespective of the electrode array used, is that the farther away the potential electrode is from the current source, the deeper the depth of investigation. The 2-D electrical resistivity survey was conducted along the six (6) traverses using the Wenner electrode array configuration. Measurements were made at sequences of electrodes interval of 5, 10, 15, 20, 25 and 30 m, respectively. Using the Wenner configuration, the four electrodes were planted into the ground, moved along each profile at a constant electrode spacing (a), and successive readings were taken. The electrode spacing was varied for deeper imaging to obtain resistivity values for a= 5 m, 10 m, 15 m, 20m, 25 m and 30m, respectively, for all six (6) CST lines. The apparent resistivity, $\rho_a$ values were obtained using the simple formula:

$$\rho_a = 2\pi aR \quad (1)$$

where R is the measured resistance in Ohms.

### 3.2 Data processing

The VES results were used to generate sounding curves for each point. This was achieved by plotting the apparent resistivity on the ordinate against half current-electrode spacing on a tracing transparent paper and curve matched. Parameters such as apparent resistivity and thickness obtained from partial curve matching were used as input data for computer iterative modelling software called WinResist. CST data obtained from the Wenner configurations were processed into apparent resistivity values, presented in note pad (.dat format), and further processed using the RES2DINV software to generate 2-D resistivity sections. The RES2DINV inversion software has proven to be effective in generating tomography images of the subsurface geology of an area.

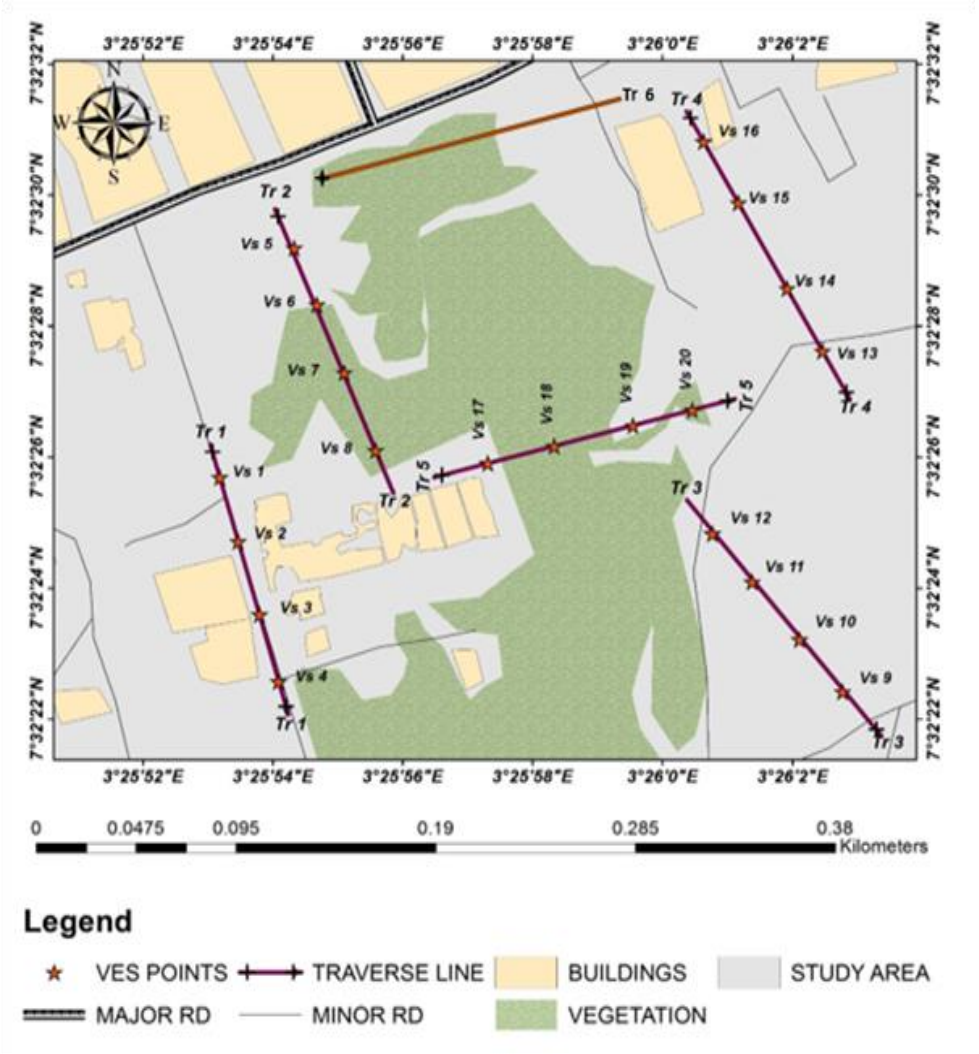


**Figure 2:** Data acquisition map of the study

## 4. Results and Discussion

### 4.1 Curve types

Three to six geoelectric layers were obtained beneath the VES points and the various curves identified include H, KH, HKH and KHKH curve types (Figure 3a to d). The three layers curve was identified beneath VES 11, 13 and 14. The four layers curve beneath VES 1, 2, 3, 4, 5, 6, 7, 8, 9, 10, 12, 15, 18, 19 and 20, five layers curve beneath VES 16, while the six layers curve was identified beneath VES 17. However, the KH type is the most common curve identified within the area. Table 1 shows the interpreted VES results with model parameters, lithology and curve type.

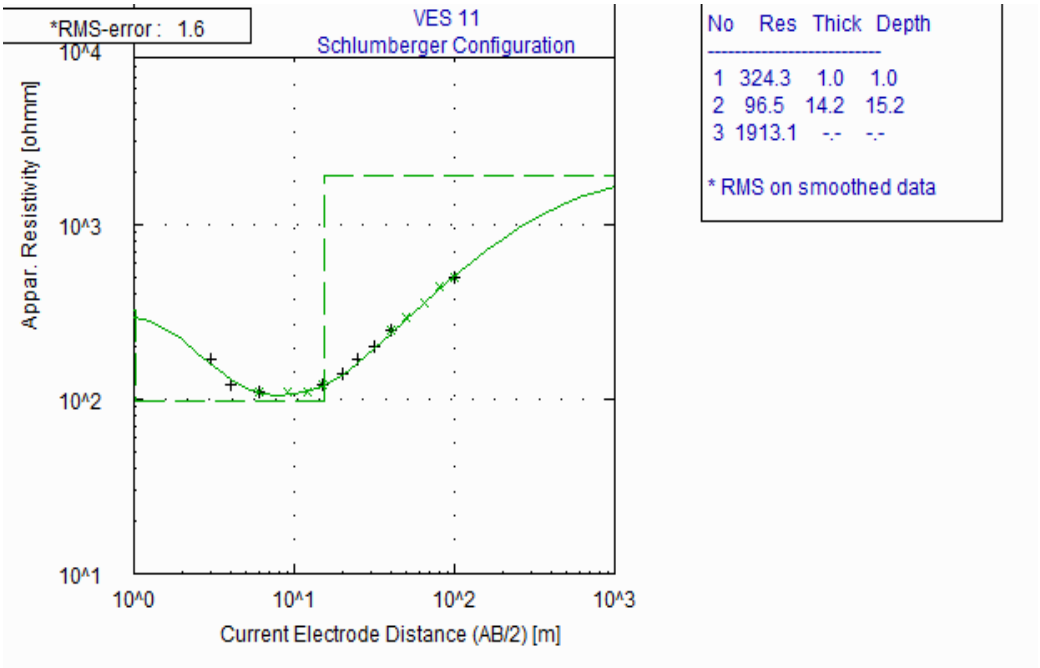


**Figure 3a:** Typical H curve type

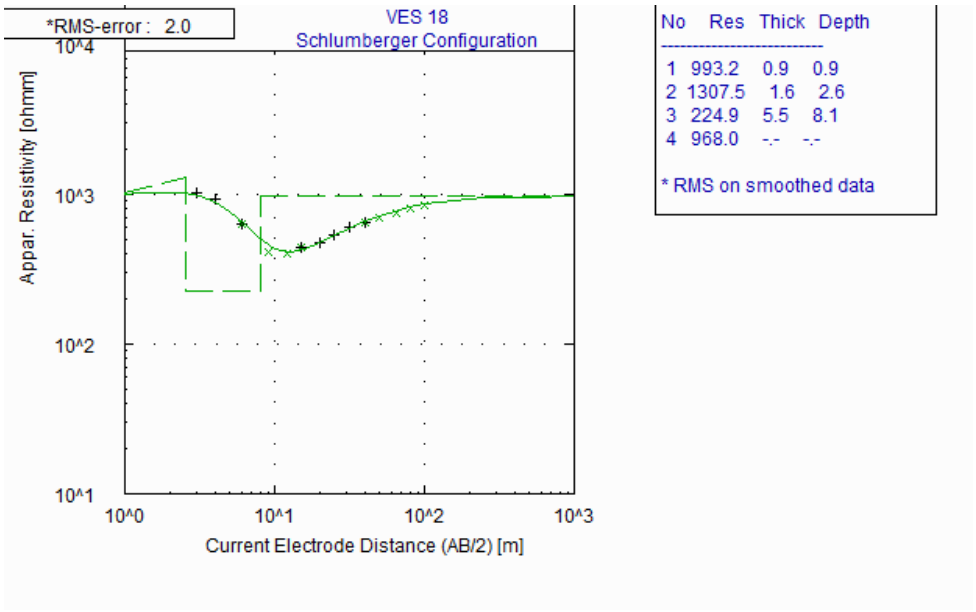


**Figure 3b:** Typical KH curve types

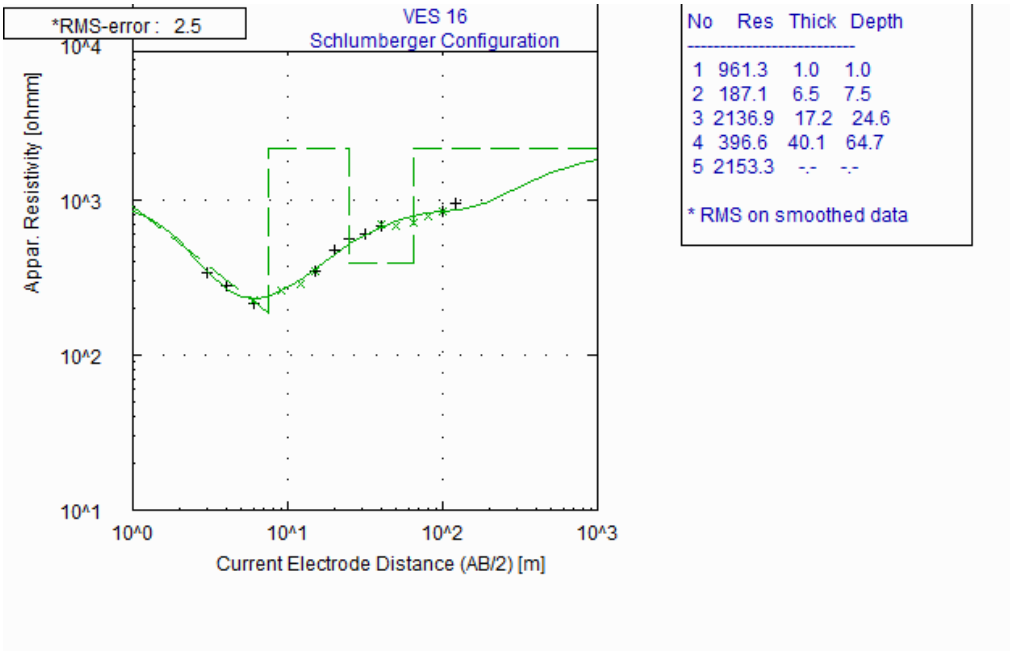


**Figure 3c:** Typical HKH curve types

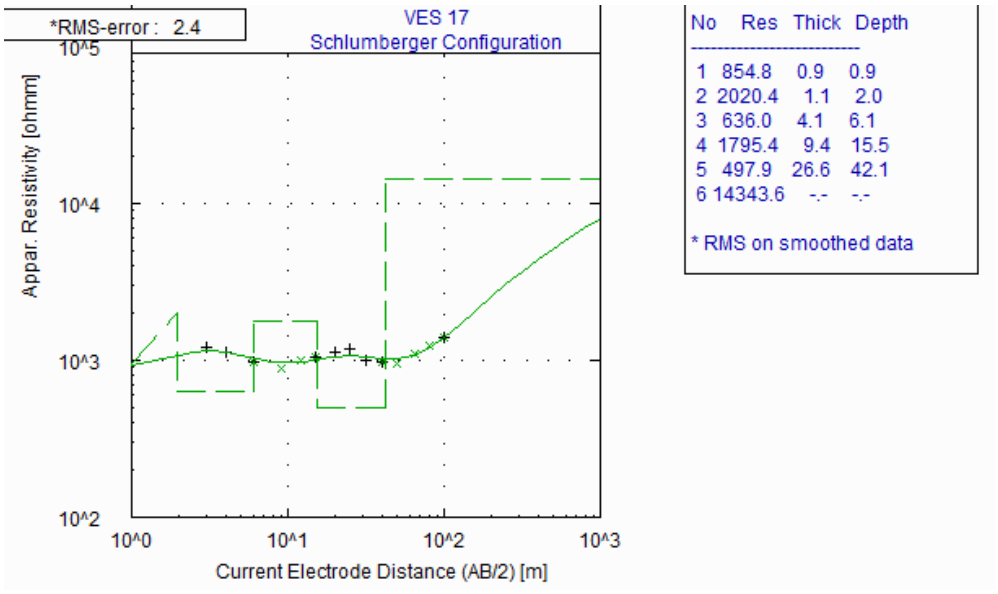


**Figure 3d**: Typical KHKH curve types

**Table 1:** Interpreted VES Results with Model Parameters, Lithology and Curve Type.

| VES | Layers | Resistivity (Ω-m) | Thickness (m) | Depth (m) | Lithology | Curve Type |
|---|---|---|---|---|---|---|
| 1 | 1 | 149 | 0.6 | 0.6 | Topsoil | KH |
| | 2 | 236 | 1.3 | 1.9 | Partly Weathered Layer | |
| | 3 | 17 | 6.2 | 8.1 | Weathered Clay | |
| | 4 | 7230 | -- | -- | Fresh Basement | |
| 2 | 1 | 532 | 0.9 | 0.9 | Topsoil | KH |
| | 2 | 628 | 1.2 | 2.1 | Partly Weathered Layer | |
| | 3 | 81 | 8.6 | 10.7 | Weathered Layer | |
| | 4 | 2021 | -- | -- | Fresh Basement | |
| 3 | 1 | 414 | 0.9 | 0.9 | Topsoil | KH |
| | 2 | 450 | 1.8 | 2.6 | Partly Weathered Layer | |
| | 3 | 63 | 8.3 | 10.9 | Weathered Layer | |
| | 4 | 1519 | -- | -- | Fresh Basement | |
| 4 | 1 | 1094 | 0.9 | 0.9 | Topsoil | KH |
| | 2 | 1733 | 1.5 | 2.3 | Partly Weathered Layer | |
| | 3 | 149 | 9.8 | 12.2 | Weathered Layer | |
| | 4 | 1472 | -- | -- | Fresh Basement | |
| 5 | 1 | 1398 | 0.8 | 0.8 | Topsoil | KH |
| | 2 | 1638 | 1.9 | 2.7 | Partly Weathered Layer | |
| | 3 | 325 | 3.6 | 6.4 | Weathered Layer | |
| | 4 | 1456 | -- | -- | Fresh Basement | |
| 6 | 1 | 1162 | 1.0 | 1.0 | Topsoil | KH |
| | 2 | 1924 | 4.8 | 5.7 | Partly Weathered Layer | |
| | 3 | 783 | 19.4 | 25.1 | Weathered Layer | |
| | 4 | 2919 | -- | -- | Fresh Basement | |
| 7 | 1 | 1407 | 1.0 | 1.0 | Topsoil | KH |
| | 2 | 1994 | 1.9 | 2.9 | Partly Weathered Layer | |
| | 3 | 850 | 21.6 | 24.5 | Weathered Layer | |
| | 4 | 8744 | -- | -- | Fresh Basement | |
| 8 | 1 | 1180 | 0.9 | 0.9 | Topsoil | KH |
| | 2 | 2082 | 1.9 | 2.8 | Partly Weathered Layer | |
| | 3 | 661 | 14.8 | 17.6 | Weathered Layer | |
| | 4 | 3086 | -- | -- | Fresh Basement | |
| 9 | 1 | 405 | 1.0 | 1.0 | Topsoil | QH |
| | 2 | 131 | 3.4 | 4.4 | Partly Weathered Layer | |
| | 3 | 54 | 5.9 | 10.3 | Weathered Layer | |
| | 4 | 710 | -- | -- | Fresh Basement | |
| 10 | 1 | 496 | 1.0 | 1.0 | Topsoil | QH |
| | 2 | 167 | 3.1 | 4.1 | Partly Weathered Layer | |
| | 3 | 45 | 18.1 | 22.2 | Weathered Layer | |
| | 4 | 741 | -- | -- | Fresh Basement | |
| 11 | 1 | 324 | 1.0 | 1.0 | Topsoil | H |
| | 2 | 97 | | 15.2 | Weathered Layer | |
| | 3 | 1913 | -- | -- | Fresh Basement | |
| 12 | 1 | 556 | 0.8 | 0.8 | Topsoil | KH |
| | 2 | 822 | 1.0 | 1.8 | Partly Weathered Layer | |
| | 3 | 73 | 6.0 | 7.8 | Weathered Layer | |
| | 4 | 1555 | -- | -- | Fresh Basement | |
| 13 | 1 | 381 | 1.0 | 1.0 | Topsoil | H |
| | 2 | 225 | 7.0 | 8.0 | Partly Weathered Layer | |
| | 3 | 3297 | -- | -- | Fresh Basement | |
| 14 | 1 | 581 | 1.0 | 1.0 | Topsoil | H |
| | 2 | 287 | 7.3 | 8.3 | Partly Weathered Layer | |
| | 3 | 2075 | -- | -- | Fresh Basement | |
| 15 | 1 | 489 | 1.0 | 1.0 | Topsoil | KH |
| | 2 | 839 | 1.6 | 2.6 | Partly Weathered Layer | |
| | 3 | 305 | 10.4 | 12.9 | Weathered Layer | |
| | 4 | 1020 | -- | -- | Fresh Basement | |

| Table 1 (Cont.): Interpreted VES Results with Model Parameters, Lithology and Curve Type. | | | | | | |
|---|---|---|---|---|---|---|
| 16 | 1 | 961 | 1.0 | 1.0 | Topsoil | HKH |
| | 2 | 187 | 6.5 | 6.5 | Weathered Layer | |
| | 3 | 2137 | 17.2 | 172 | Fresh Basement | |
| | 4 | 397 | 40.1 | 64.7 | Fractured Basement | |
| | 5 | 2153 | -- | -- | Fresh Basement | |
| 17 | 1 | 855 | 0.9 | 0.9 | Topsoil | KHKH |
| | 2 | 2020 | 1.1 | 2.0 | Laterite | |
| | 3 | 636 | 4.1 | 6.1 | Partly Weathered Layer | |
| | 4 | 1795 | 9.4 | 15.5 | Fresh Basement | |
| | 5 | 498 | 26.6 | 42.1 | Fractured Basement | |
| | 6 | 14343 | -- | -- | Fresh Basement | |
| 18 | 1 | 993 | 0.9 | 0.9 | Topsoil | KH |
| | 2 | 1308 | 1.6 | 2.6 | Laterite | |
| | 3 | 225 | 5.5 | 8.1 | Weathered Layer | |
| | 4 | 968 | -- | -- | Fractured Basement | |
| 19 | 1 | 685 | 1.0 | 1.0 | Topsoil | KH |
| | 2 | 889 | 1.4 | 2.4 | Partly Weathered | |
| | 3 | 179 | 4.9 | 7.3 | Weathered Layer | |
| | 4 | 5084 | -- | -- | Fresh Basement | |
| 20 | 1 | 808 | 0.8 | 0.8 | Topsoil | KH |
| | 2 | 831 | 1.1 | 1.9 | Partly Weathered | |
| | 3 | 90 | 2.6 | 4.4 | Weathered Layer | |
| | 4 | 2643 | -- | -- | Fresh Basement | |

### 4.2 Geo-electrical section

Figure 4(a to e) represents the geoelectric section along the five profiles. Geo-electric Section along AA$^{I}$ (Figure 4a) represents the geoelectric section along profile 1. The geoelectric section relates VES 1, 2, 3, and 4 positions at 138 m, 145 m, 150 m and 170 m. The geoelectric section reveals three to four geoelectric layers: topsoil, sand, clay/sandy clay, and sand formation. The first layer represents the topsoil with resistivity values ranging from 149 to 1094 Ωm with thickness values that vary from 0.6 to 0.9 m. The second layer is composed of the partly weathered layer with resistivity values ranging from 236 to 1733 Ωm with thickness values varying from 1.2 to 1.8 m within the depth range of 1.9 to 2.6 m. The third layer constitutes a weathered layer. It has resistivity and thickness values that vary between 63 to 149 Ωm and 8.3 to 9.8 m within depths that vary from 10.7 to 12.2 m, respectively but is composed of clay on VES 1 with resistivity and thickness values of 17 Ωm and 6.2 m. The fourth represents fresh basement rock having resistivity values that vary between 1472 to 7230 Ωm. This fourth geoelectric layer's thickness could not be determined because of current electrode terminate at this region.

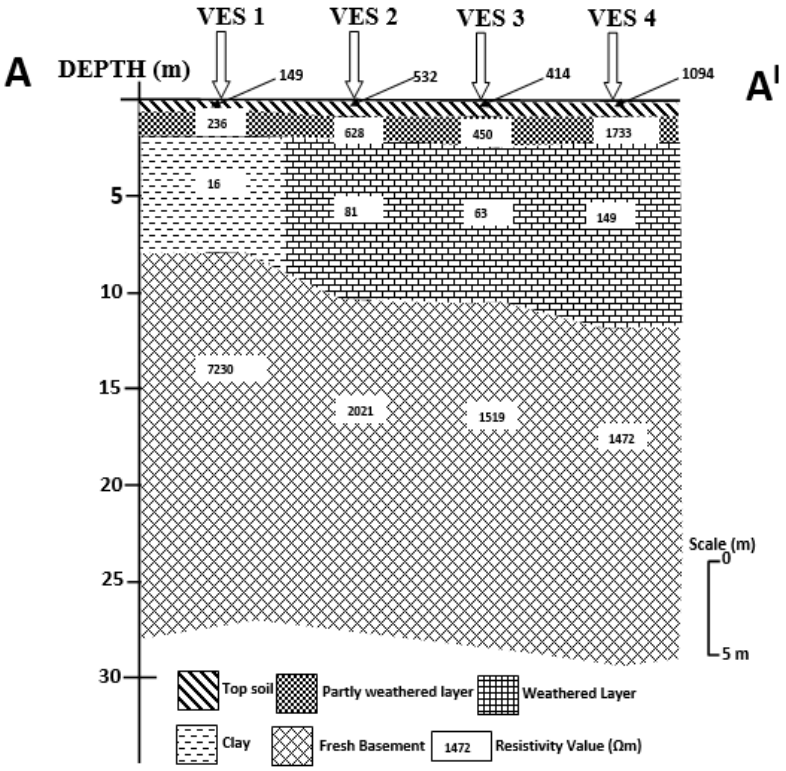


**Figure 4a:** Geo-electric Section along A – A$^{I}$

Geo-electric Section along BB$^{I}$ revealed the geoelectric section along profile 2 (Figure 4b). The geoelectric section consists of VES 5, 6, 7, and 8 positioning at 120 m, 130 m, 140 m, and 150 m, respectively. The first layer represents the topsoil that has a resistivity values ranging from 1162 to 1407 Ωm with thickness values varying from 0.8 to 1.0 m.The second layer is composed of the partly weathered layer with resistivity values ranging

from 1638 to 2082 Ωm with thickness values varying from 1.9 to 4.8 m within the depth range of 2.7 to 5.7 m.The third layer constitutes a weathered layer with resistivity and thickness values ranging from 325 to 850 Ωm and 3.6 to 21.6 m within a depth of 6.4 to 25.1 m.The fourth layers represents fresh basement rock having resistivity values varying from 1456 to 8744 Ωm. This fourth geoelectric layer's thickness could not be determined because of current electrode terminate at this region.

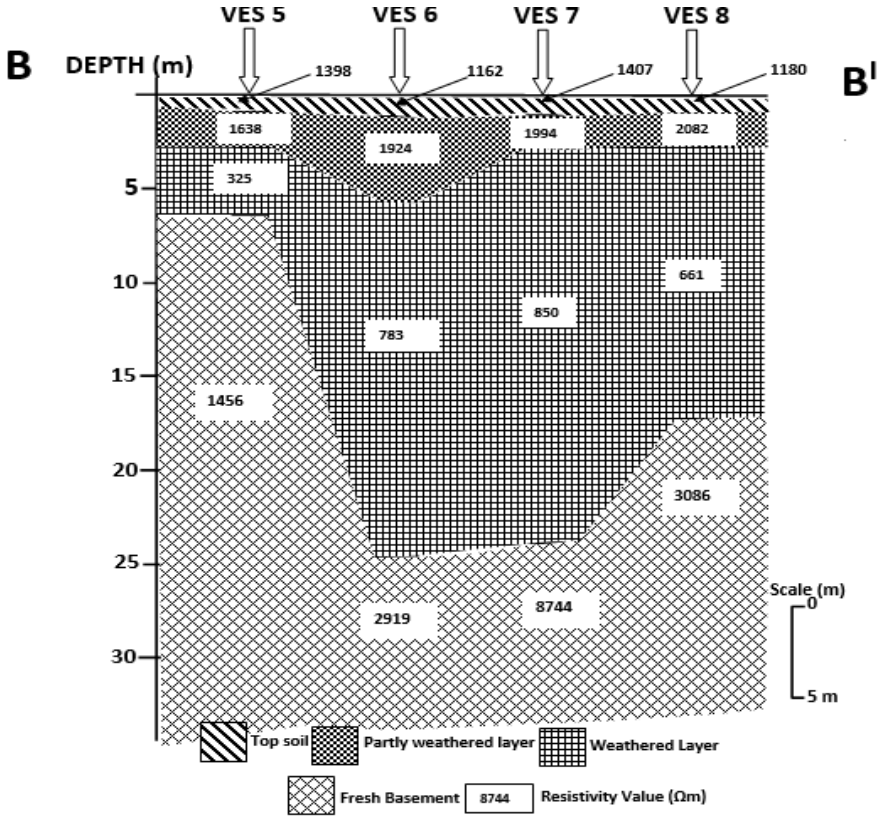


**Figure 4b:** Geo-electric Section along B – B$^{I}$

Geo-electric Section along CC$^{I}$ (Figure 4c) represents the geoelectric section along profile 3. The geoelectric section consists of VES 9, 10, 11 and 12 positioned at 50 m, 60 m, 70 m, and 80 m, respectively. The topsoil has resistivity values ranging from 324 to 556 Ωm with thickness values varying from 0.8 to 1.0 m. The second layer composed of a weathered and partly weathered layer with resistivity values ranging from 187 to 839 Ωm and thickness values varying from 1.6 to 7.3 m within the depth range of 2.6 to 8.3 m. The third layer represents weather layer with resistivity and thickness values ranging from 45 to 73 Ωm and 5 to 14 m. The fifth geoelectric layer represents fresh basement with resistivity and thickness values ranging from 710 to 1913 Ωm..

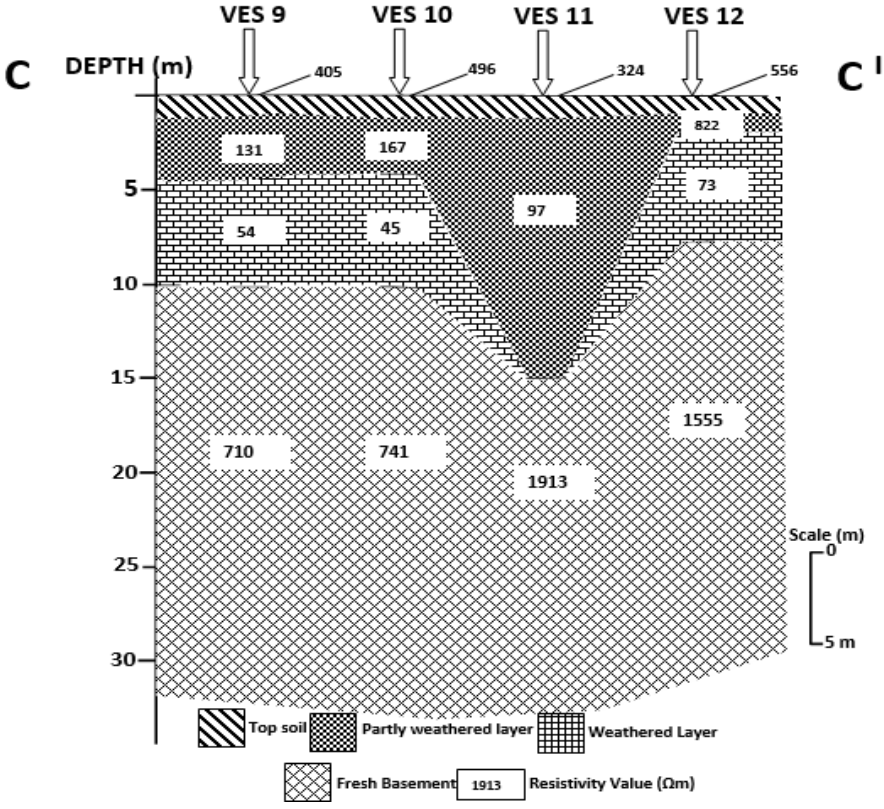


**Figure 4c:** Geo-electric Section along C-CI

Geo-electric Section along DD$^{I}$ representsthe geoelectric section along profile 4 (Figure 4d) relating VES 13, 14, 15 and 16 positions at 80 m, 85 m, 90 m and 95 m. The first layer represents the topsoil, it has resistivity values ranging from 99 to 109 Ωm with thicknesses varying from 0.6 to 1.0 m.The topsoil is composed of sand. The second geoelectric layer is composed of a weathered and partly weathered layer with resistivity values ranging from 187 to 839 Ωm with thickness values varying from 1.6 m to 7.3 m within the depth range of 2.6 m to 8.3 m. The third geoelectric layer represents fresh basement with resistivity and thickness values varying from 2075 Ωm to 3297 Ωm but compose of weathered layer on VES 15 having resistivity and thickness values of 305 Ωm and 10.4 m within the depth of 12.9 m respectively. The fourth geoelectric represents fresh basement with resistivity value of 1020 Ωm, but is composed of the fractured basement on VES 16 having resistivity and thickness values of 397 Ωm and 40.1 m within the depth of 64.7 m. The fifth geoelectric layer represents a fresh basement and has a resistivity value of 2153 Ωm.

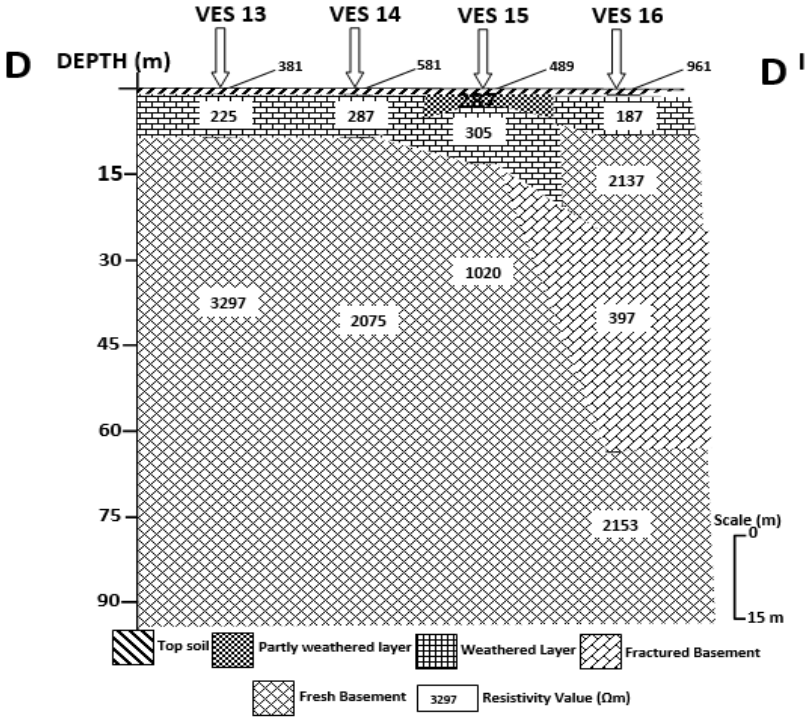


**Figure 4d:** Geo-electric Section along D-D$^{I}$

Geoelectric section along EE$^{I}$ representing profile 5 (Figure 4e) consists of VES 17, 18, 19, and 20 positioned at 70 m, 90 m, 100 m and 110 m, respectively. The topsoil has resistivity values ranging from 685 to 993 Ωm with thickness values varying from 0.9 to 1.0 m. The second layer is composed of the partly weathered layer with resistivity values ranging from 831 to 2020 Ωm with thickness values varying from 1.1 to 1.6 m within the depth range of 1.9 to 2.6 m. The third layer represents weathered layer with resistivity and thickness values varying from 90 to 225 Ωm and 2.6 to 5.5 m within the depth range of 4.4 m to 8.1 m, but composed partly weathered layer on VES 17 with resistivity and thickness values of 636 Ωm and 4.1 m within the depth of 6.1 m. The fourth geoelectric represents fractured basement (beneath VES 18) and fresh basement with resistivity values ranging from 968 Ωm to 5084 Ωm. The fifth geoelectric layer is composed of fractured basement on VES 17 having resistivity and thickness values of 498 Ωm and 26.6 m within the depth of 42.1 m. The sixth geoelectric layer represents a fresh basement and has a resistivity value of 14344 Ωm.

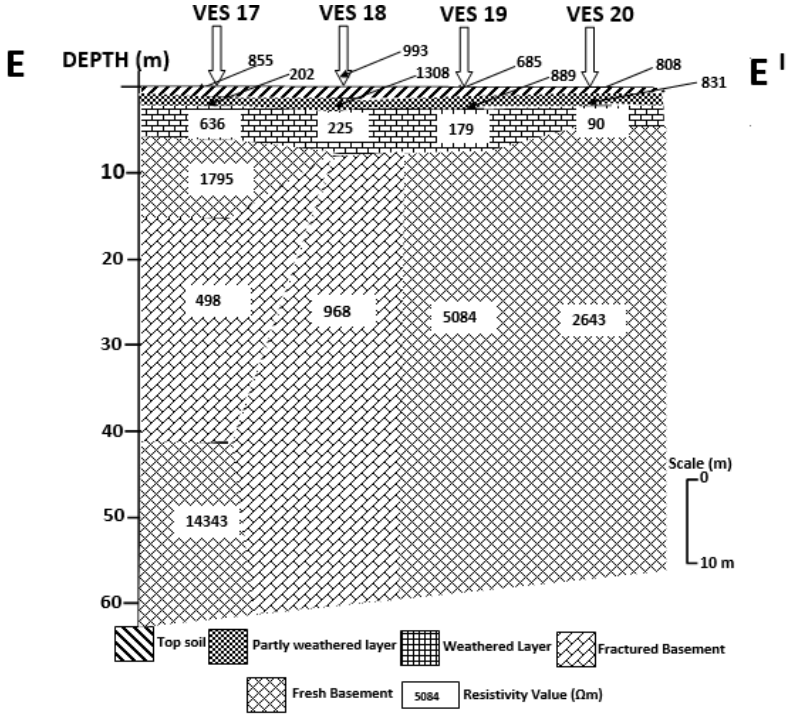


**Figure 4e:** Geo-electric Section along E-E$^{I}$

### 4.3 2-D Resistivity section along traverse one

The 2-D resistivity section along traverse 1 is presented in Figure 5. The section indicates a total spread length of 200 m and maximum depth of 17.3 m wasinvestigated. The resistivity section shows that three zones/regions are distinctively mapped with resistivity values that ranges from 31.5 – 8754 Ωm. The subsurface layer is composed of weathered and partly weathered layer from the surface to depth range of about 10 m - 17.3 m. The weathered layer (70 Ωm - 157 Ωm) was identified at lateral distance of about 10-35 m and 95 m - 175 m as the second geoelectric layer and extend to depth of 17.3 m. The partly weathered layer is identified at lateral distance of about 35 m - 90 m and extend to depth range of about 10 m - 17.3 m respectively. The third geo-electric layer composed of fresh basement (1754 Ωm - 8754 Ωm) and extends from depth of about 10.0 m - 17.3 m. The weathered layer represent the aquifer unit suitable for hydrogeologic purpose or groundwater exploration in the area.

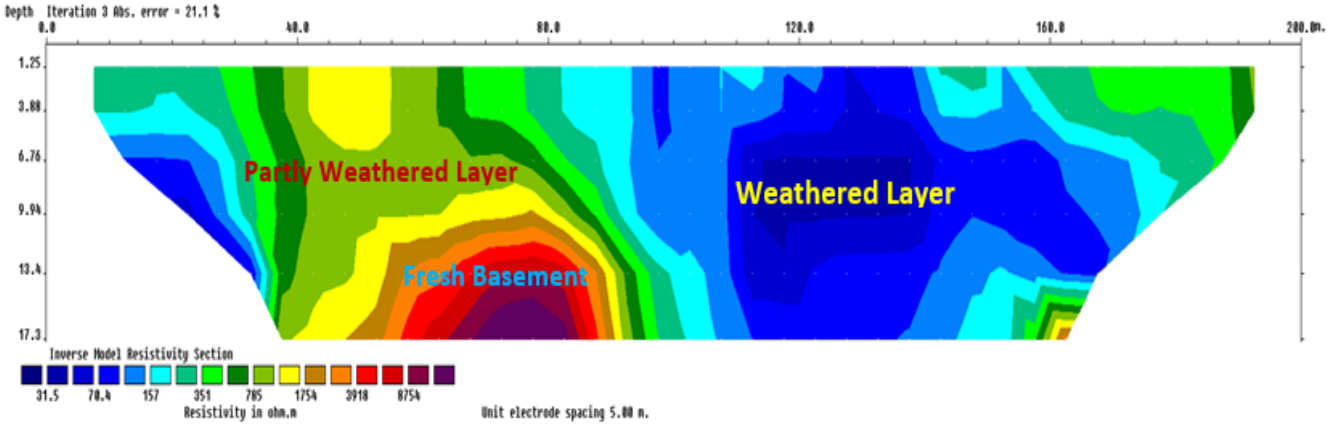


**Figure 5:** 2-D Resistivity Section along Profile 1

### 4.4 2-D Resistivity section along traverse two

The 2-D resistivity section along traverse 2is presented in Figure 6. The section indicate total spread length of 150 m and maximum depth of 19.8 m wasinvestigated. The resistivity section shows resistivity values that ranges from 134 – 23197 Ωm. From the inverted section, the topsoil has resistivity values that range from 134 – 2550 Ωm. Below the topsoil, the subsurface layer composes of weathered and partly weathered layer from the surface to depth range of about 1.25 m - 17.0 m. The partly weathered layer (1222 Ωm -2550 Ωm) was identified at lateral distance of about 5-40 m from depth of about 1.25 - 9.26 m. The weathered layer represents the aquifer unit. The third geo-electric layer is composed of fresh basement (5324 Ωm -23197 Ωm) identified at depth of about 17 – 19.8 m.

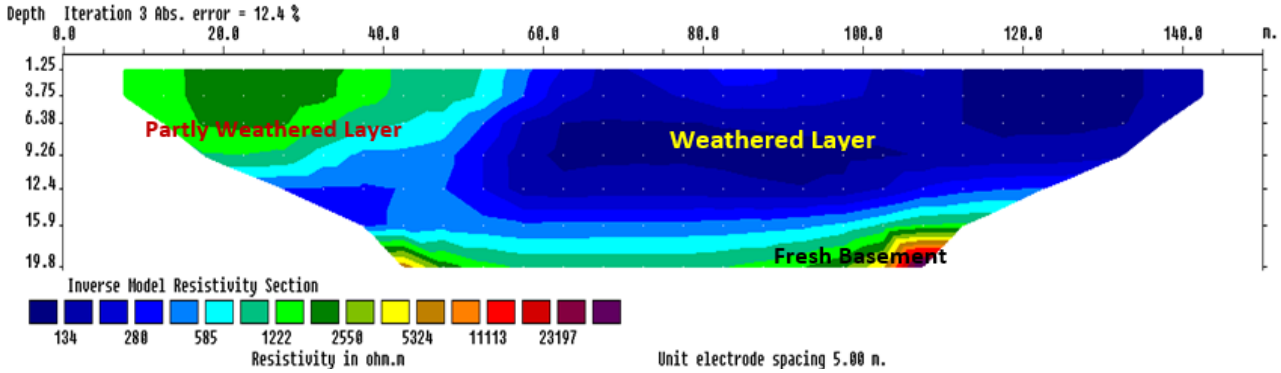


**Figure 6:** 2-D Resistivity Section along Profile 2

### 4.5 2-D Resistivity section along traverse three

The 2-D resistivity section along traverse 3is presented in Figure 7. The section indicate total spread length of 150 m and maximum depth of 19.8 m wasinvestigated. The resistivity section shows resistivity values that ranges from 8.28 – 122718 Ωm. From the inverted section, the topsoil has resistivity values that range from 32.6 – 2002 Ωm. Below the topsoil, the subsurface layer is composed of weathered and partly weathered layer from the surface to depth range of about 6.0 m - 12.0 m and has resistivity values that range from 48 – 2002 Ωm. The weathered layer (48 Ωm - 129 Ωm) is identified at lateral distance of about 47 - 85 m from depth of about 1.25 –10.0 m. The third geo-electric layer is composed of fresh basement (7892 Ωm - 122710 Ωm) from depth of about 6.38 – 19.8 m.

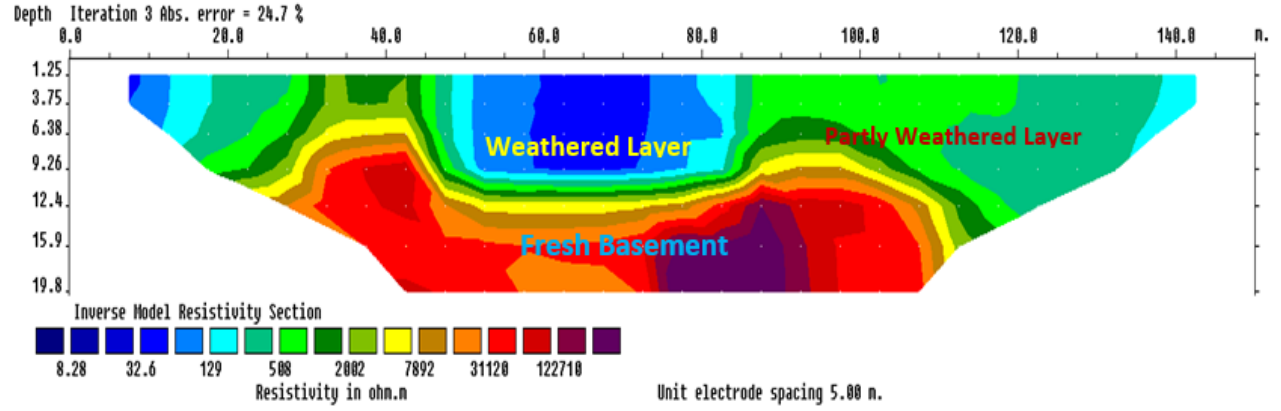


**Figure 7:** 2-D Resistivity Section along Profile 3

### 4.6 2-D Resistivity section along traverse four

The 2-D resistivity section along traverse 4 is presented in Figure 8. The section indicate total spread length of 150 m and maximum depth of 15.9 m wasinvestigated. The resistivity section shows resistivity values that ranges from 78.7 – 10770 Ωm. From the inverted section, the topsoil has resistivity values that range from 159 – 5333 Ωm. The second layer is composed of weathered layer (at lateral distance of 0 – 105 m) and partly weathered layer (at lateral distance of 115 – 150 m) from the surface to depth range of about 1.25 m - 10 m with resistivity values that range from 159 – 2641 Ωm. The weathered layer (thin) represent aquifer unit. The third geo-electric layer is composed of fresh basement (2641 Ωm - 10770 Ωm) from depth of about 6.38 – 15.9 m. Suspected fractured is identified at lateral distance of 105 – 115 m along this traverse. The fractured basement represents aquifer unit for groundwater development.

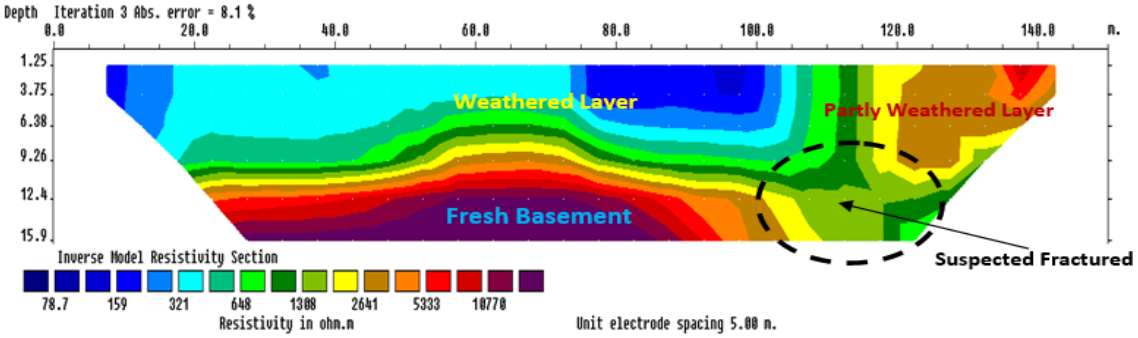


**Figure 8:** 2-D Resistivity Section along Profile 4

### 4.7 2-D Resistivity section along traverse five

The 2-D resistivity section along traverse 5is presented in Figure 9. The section indicate total spread length of 200 m and maximum depth of 19.8 m wasinvestigated. The resistivity section shows resistivity values that ranges from 215 – 64874 Ωm. From the inverted section, the topsoil has resistivity values that range from 215 – 2472 Ωm. The second layer is composed of weathered layer (at lateral distance of 45 – 190 m) and partly weathered layer (at lateral distance of 5 – 45 m) from the surface to depth range of about 1.28 - 10 m with resistivity values that range from 215 – 2472 Ωm. The weathered layer (thin) represent aquifer unit. The third geo-electric layer is composed of fresh basement (12584 Ωm - 64874 Ωm) from depth of about 10.0 – 19.8 m, but represent fractured basement (485 – 1095 Ωm) or thick weathered layer at lateral distance of about 45 – 85 m along this traverse. The fractured basement is also identified on VES 17 conducted at lateral distance of 70 m along the traverse line.

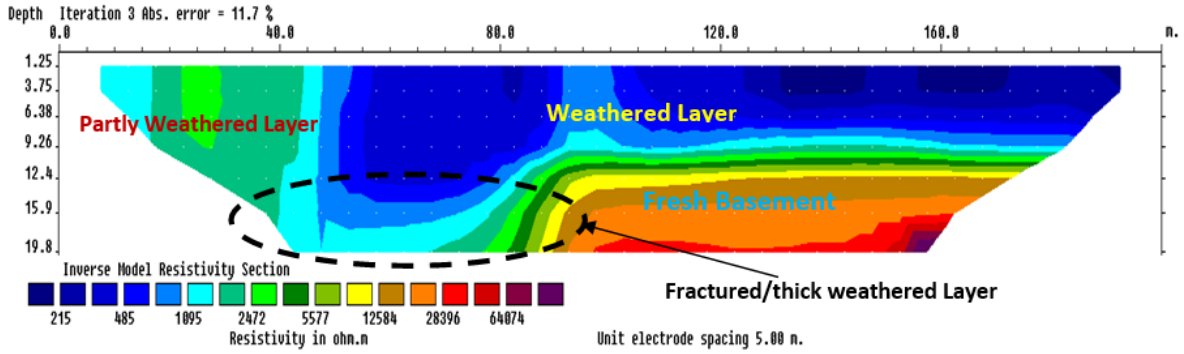


**Figure 9:** 2-D Resistivity Section along Profile 5

### 4.8 2-D Resistivity section along traverse six

The 2-D resistivity section along traverse 6is presented in Figure 10. The section indicate total spread length of 200 m and maximum depth of 19.8 m wasinvestigated. The resistivity section shows resistivity values that ranges from 239 – 62850 Ωm. the topsoil has resistivity values that range from 239 – 1174 Ωm. The second layer is composed of weathered and partly weathered layer from depth range of about 1.25– 12.4 m having resistivity values that range from 530 – 1174 Ωm. The weathered layer (thin) represents aquifer unit. The third geo-electric layer is composed of fresh basement (2603 Ωm - 62850 Ωm) from depth range of about 10.0 – 19.8 m.

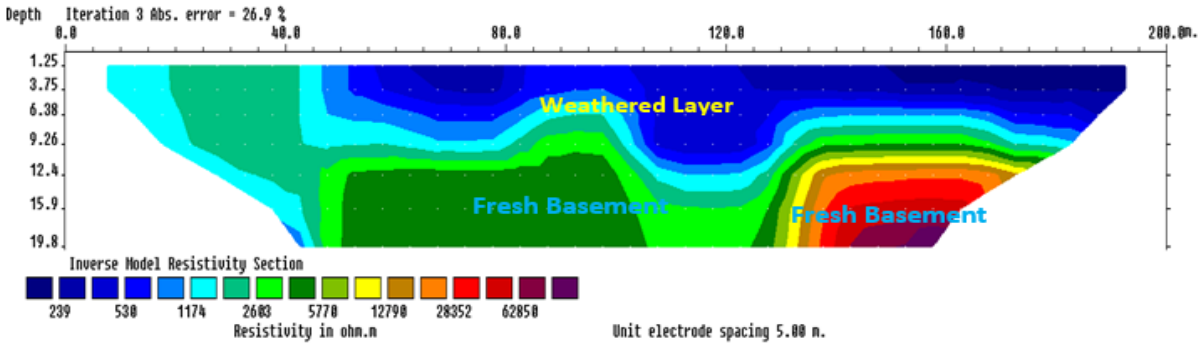


**Figure 10:** 2-D Resistivity Section along Profile

## 5. INTEGRATION OF RESULTS

### 5.1 Integration of VES and CST along Traverse 3

Figure 11 represents the correlation panel of the VES and CST results along traverse 3 for proper lithology identification. From the section, there is good correlation of the VES with the CST as both techniques identified the second geoelectric layer as partly weathered and weathered layer. The third geoelectric layer is identified as weathered layer while the fourth geoelectric layer were both delineated as fresh basement.

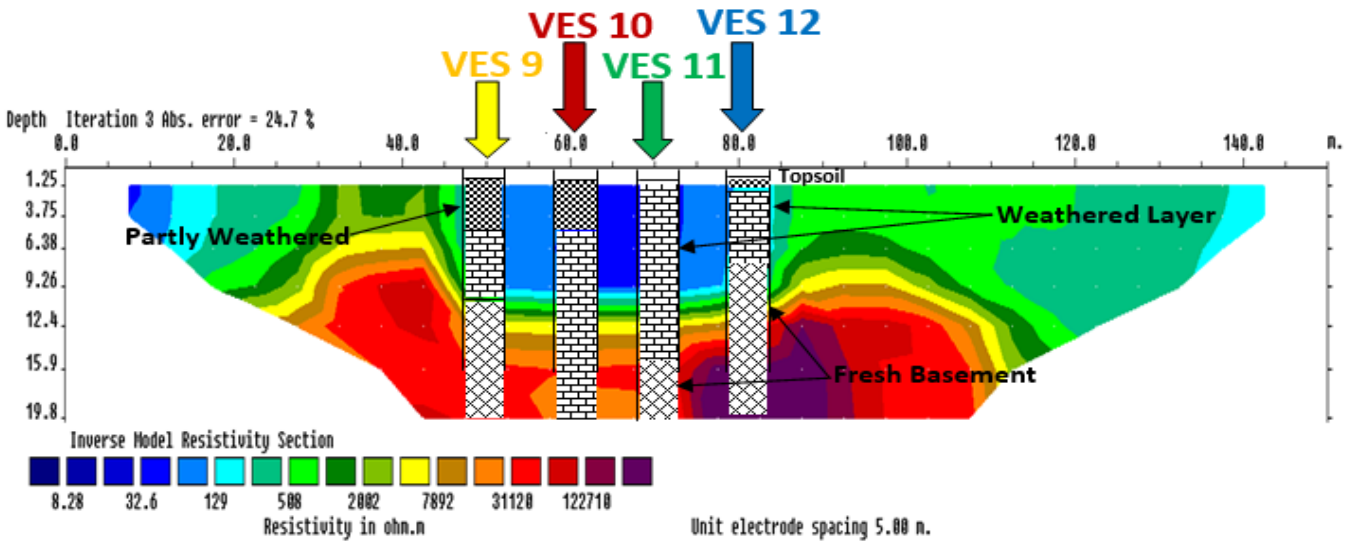


**Figure 11:** Correlation of VES and CST Results along Traverse 3

### 5.2 Integration of VES and CST along Traverse 5

Figure 12 represents the correlation panel of the VES and CST along traverse 5. From the section, there is good correlation of the VES with the CST. The fractured basement identified on the VES 17 and 18 corresponds well with the fractured identified on the 2-D section as lateral distance of 70 and 90 m respectively. This represents suitable location where groundwater can be tapped.

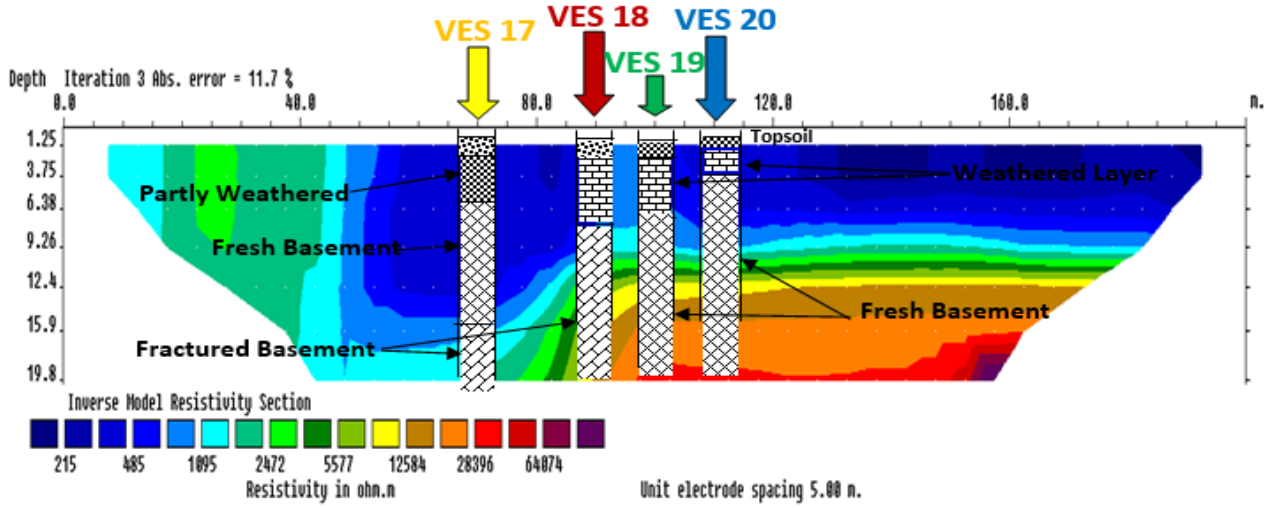


**Figure 12:** Correlation of VES and CST Results along Traverse 5.

### 5.3 Reflection coefficient to determine the reliability of VES techniques

Some researchers have used values of reflection coefficient to determine the reliability of VES method (Olorunfemi et al., 1999). The Lower the value of the coefficient, the more promising is the fractured layer for grandwater potential. Table 2 Shows the values of Computed Reflection Coefficient for some suspected VES points that are selected on the basis of their Resistivity values and Thickness. The Table shows that VES 5, 6, 8, 15, 18 are promising

**Table 2:** The values of computed reflection coefficient for some suspected VES points

| VES Points | Apparent Resistivity Value $\varrho_1$, $\varrho_2$ (Ωm) | Computed Reflection Coefficient | Groundwater Potential |
|---|---|---|---|
| 2 | 81.3, 2021.4 | 0.922 | Poor |
| 4 | 148.5,1472.2 | 0.817 | Poor |
| 5 | 325.3, 1455.7 | 0.635 | Very good |
| 6 | 783.4, 2919.4 | 0.577 | Very good |
| 7 | 849.8, 87441 | 0.823 | Poor |
| 8 | 661.1, 3085.5 | 0.647 | Very good |
| 11 | 96.5, 1913.1 | 0.904 | Poor |
| 13 | 225.3, 3296.8 | 0.872 | Poor |
| 14 | 286.5, 2074.8 | 0.757 | Good |
| 15 | 305.3, 1020.2 | 0.539 | Very good |
| 18 | 224.9, 968.0 | 0.623 | Very good |

## 6. Conclusions

The rock that underlain the study area are granite and gneisses such rock have been found to be overlain by thick overburden, which can be good for shallow water. Electricity Resistivity survey has shown that there are five Geoelectric Layers, Topsoil, Partially Weathered Layer, Fractured Basement, and Fresh Basement. The fracture zone have been found to be the most promising for groundwater accumulation. Consideration of the thickness of overburden, resistivity of fracture zone and the computed values of reflection coefficient were used to identify 5 promising VES points for groundwater accumulation. Electrical Resistivity Survey has been successfully carried out for groundwater exploration in the study area.

Similar study can be carried out in other Basement Complex terrains in Nigeria. However integrated geophysical methods should be employed. The study should be followed with ground-truthing involving drilling of Boreholes and this will assist in determining the effectiveness or otherwise of geophysical method for groundwater exploration in basement complex terrains.

## References


Abiola, O., Enikanselu, P. A., and Oladapo, M. I., 2009. Groundwater potential and aquifer protective capacity of overburden units in Ado-Ekiti, southwestern Nigeria. International Journal of Physical Sciences, 4(3), Pp. 120-132.

Adebiyi, A.D., Ilugbo, S.O., Bamidele, O.E., Egunjobi, T., 2018. Assessment of aquifer vulnerability using multi- criteria decision analysis around akure industrial estate, Akure, Southwestern Nigeria. J Eng Res Rep 3(3), Pp. 1–13

Adebo, B.A., Ilugbo, S.O., Jemiriwon, E.T., Ali, A.K., Akinwumi, A.K., Adeniken, N.T., 2022 Hydrogeophysical Investigation Using Electrical Resistivity Method within Lead City University Ibadan, Oyo State, Nigeria. Int J Earth Sci Knowl Appl 4(1), Pp. 51–62

Adebo, B.A., Layade, G.O., Ilugbo, S.O., Hamzat, A.A., Otobrise, H.K., 2019. Mapping of subsurface geological structures using ground magnetic and electrical resistive ty methods within lead city university Southwestern Nigeria. Kada J Phys 2(2): Pp. 64–73

Adebo, A.B., Ilugbo, S.O., Oladetan, F.E., 2018. Modeling of groundwater potential using Vertical Electrical Sounding (VES) and multi-criterial analysis at Omitogun Housing Estate, Akure, Southwestern Nigeria. Asian J Adv Res Rep 1(2), Pp. 1–11

Ajibade, A. C., 1976. Provisional classification and correlation of the schist belts in Northwest Nigeria. In: Kogbe, C.A. (ed) Geology of Nigeria. Elizaberthan Pub. Co., Surulere, Lagos, Nigeria. Pp. 85-90.

Ajibade, A.C., 1980. Geotectonic evolution of the Zungeru region, Nigeria. Unpub. Ph.D. Thesis, Univ. Wales, Aberystwyth, 320.

Ayolabi, E. A., Adedeji, J. K., and Oladapo, I. M., 2004. A geoelectric mapping of Ijapo, Akure Southwest Nigeria and its hydrogeological implications. Global Journal of Pure and Applied Sciences, 10 (3), Pp. 441-446.

Bawallah M.A, Adebayo A.E., Ilugbo S.O., Adewumi O.A, Ayodele T., Olutomilola O.O., 2024. Ground Water Sustainability in A Crystalline Rock Environment Using Electrical Resistivity and Mcda Approach in The Federal Polytechnic Ado-Ekiti, Ekiti State, Nigeria. Earth Sciences Pakistan, 8(1), Pp. 05-18.

Bawallah, M.A., Adiat, K.A.N., Akinlalu, A.A., Ilugbo, S.O., Akinluyi, F.O., Ojo, B.T., Oyedele, A.A., Bamisaye, O.A., Olutomilola, O.O., Magawata, U.Z., 2021a Resistivity contrast and the phenomenon of geophysical anomaly in ground water exploration in a crystalline basement environment Southwestern Nigeria. Int J Earth Sci Knowl Appl 3(1), Pp. 23–36

Bawallah, M.A., Adiat, K.A.N., Akinlalu, A.A., Ilugbo, S.O., Akinluyi, F.O., Benjamin, O.O., Oyedele, A.A., Omosuyi, G.O., Aigbedion, I., 2021b. Groundwater sustainability and the divergence of rock types in a typical crystalline basement complex region Southwestern Nigeria. Turkish J Geosci 2 (1), Pp. 1–11. https:// doi. org/ 10. 48053/ turkg eo. 777217

Bawallah, M.A., Ilugbo, S.O., Aina, A.O., Olufemi, B., Akinluyi, F.O., Ojo, B.T., Oyedele, A.A., Olasunkanmi, N.K., 2020a. Hydrogeophysical studies of central Kwara state basement complex of Nigeria. Int J Earth Sci Knowl Appl 2(3), Pp. 146–164

Bawallah, M.A., Ofomola, M.O., Ilugbo, S.O., Aina, A.O., Olaogun, S.O., Olayiwola, K.O., Awoniran, D.R., 2020b. Effect of Lineament and drainage orientation on groundwater potential of moroarea central Kwara state Nigeria. Indian J Sci Technol 13(10), Pp. 1124 1134

Bawallah, M.A., Adebayo, A., Ilugbo, S.O., Olufemi, B., Alagbe, O.A., Olasunkanmi, K.N., 2018a. Evaluation of groundwater prospect in a clay dominated environment of central Kwara state Southwestern Nigeria. Int J Adv Eng Res Sci 5(6), Pp. 45–56

Bawallah, M.A., Aina, A.O., Ilugbo, S.O., Ozegin, K.O., Olasunkanmi, K.N., 2018b. Evaluationof groundwater yield capacity using darzarrouk parameter of central Kwara state, Southwestern Nigeria. Asian J Geol Res 1(1), Pp. 1–13

Barongo, J. O. and Palacky, G. J., 1991. Investigations of electrical properties of weathered layers in the Yala area, western Kenya, using resistivity soundings. Geophysics, 56 (1), Pp. 133 138 doi:10.119 0/1.1442949

Cooray, P. G., 1972. One-inch geological map series no. 28, Puttalam. Ceylon Geol. Surv. Dept.

Dada, S. S, Birck, J. L., Lancelot, J. R. and Rahaman, M. A., 1993. Archaean migmatite-gneiss complex of Northcentral Nigeria: its geochemistry, petrogenesis and evolution. International Colloquim on African Geology, Mbabane, Swaziland (1), Pp. 97-102.

Dada, S.S., and Rahaman, M.A., 1995. Archean-Lower Paleozoic Crustal evolution in Nigeria. African Geoscience Review, 2, Pp. 219-225.

Ilugbo, S.O., Adebiyi, A.D., 2017. Intersection of Lineaments for groundwater prospect analysis using satellite remotely sensed and aeromagnetic dataset around Ibodi, Southwestern Nigeria. Int J of Phys Sci 12 (23), Pp. 329–353

Ilugbo, S.O., Ozegin, K.O., 2018a. Significances of Deep Seated Lineament in Groundwater Studies around Ilesha, Southwestern Nigeria. Asian J Geol Res 1(1), Pp. 1–16

Ilugbo, S.O., Adebiyi, A.D., Olomo, K.O., 2018b. Modeling of groundwater yield using gis and electrical resistivity method in a basement complex terrain, Southwestern Nigeria. J Geog EnvironEarth Sci Intern 16(1), Pp. 1–17

Ilugbo, S.O., Adebo, B.A., Olomo, K.O., Adebiyi, A.D., 2018c. Application of Gis and multi criteria decision analysis to geoelectric parameters for modeling of groundwater potential around ilesha, Southwestern Nigeria. Eur J Acad Essays 5(5), Pp. 105–123

Ilugbo, S.O., Edunjobi, H.O., Alabi, T.O., Ogabi, A.F., Olomo, K.O., Ojo, O.A., Adeleke, K.A., 2019. Evaluation of Groundwater Level Using Combined Electrical Resistivity Log with Gamma (Elgg) around Ikeja, Lagos State, Southwestern Nigeria. Asian J Geol Res 2(3), Pp. 1–13

Ilugbo, S.O., Adewoye, O.E., Aladeboyeje, A.I., Magawata, U.Z., Oyedele, A.A., Alabi, T.O., Owolabi, D.T., Adeleke, K.A., Adebayo, S.O., 2020. Modeling of groundwater potential using remotely sensed data within Akure metropolis Ondo State Southwestern Nigeria. Applied J Phys Sci 2(3), Pp. 38–54. https:// doi. org/ 10. 31248/ AJPS2 019. 028

Ilugbo, S.O., Aigbedion, I., Ozegin, K.O., Bawallah, M.A., 2023a. Assessment of groundwater occurrence in a typical schist belt region in Osun state, southwestern Nigeria using VES, aeromagnetic dataset, remotely sensed data and MCDA approaches. Sustain. Water Resourc. Manag. 9, Pp. 29. https://doi.org/10.1007/s40899- 022-00810-1.

Ilugbo, S.O., Aigbedion, I., Ozegin, K.O., 2023b. Structural mapping for groundwater occurrence using remote sensing and geophysical data in Ilesha Schist Belt, Southwestern Nigeria. Geology, Ecology, and Landscapes. https://doi.org/10.1080/ 24749508.2023.2182063.

Jatau B. S., Patrick N. O., Baba A. and Fadele S. I., 2013. The use of vertical electrical sounding (VES) for subsurface geophysical investigation around Bomo area, Kaduna state, Nigeria," IOSR journal of engineer ing, 3 (1), Pp. 10- 15.

Manda, A. K., Mabee, S. B and Boutt, D. F., 2006. Characterising fractured crystalline bedrock aquifers using hydrostructural domains in the

Nashoba Terrain, Eastern Massachusetts. Geological society of America, Philadelphia, Pennsylvania, Pp. 22-25.

Mc Curry, P., 1976. The geology of the Precambrian to lower Palaeozoic Rocks of NorthernNigeria –A review In: Kogbe C.A (ed) Geology of Nigeria. Elizabethan Publishers, Lagos, Pp. 15-39.

Olayinka, A.I. and Olorunfemi, M.O., 1992. Determination of Geoelectric Characteristics in Okene Area and Implications for Borehole Siting. Journal of Mining and Geology, 28, Pp. 403-411.

Olorufemi, M.O., Ojo J.S. and Akintunde O.M. 1999. Hydrogeophysical evaluation of the groundwater potentials of the Akure metropolis, South western Nigeria, Journal of Minning and Geology, 35 (2), Pp. 201-228.

Oyawoye, M. O., 1972. The basement complex of Nigeria in African Geology edited by T. F. J Dessau Vagie and Whiteman, A.J. Whiteman. University of Ibadan Press, Pp. 66-102.

Oyawoye, M. O., 1964. The Geology of the Nigerian basement complex: Journal of the Nigerian Mining, Geological and Metallurgical Society, 1, Pp. 87-482.

Ozegin, K.O., Ilugbo, S.O., Ogunseye, T.T., 2023. Groundwater exploration in a landscape with heterogeneous geology: an application of geospatial and analytical hierarchical process (AHP) techniques in the Edo north region, in Nigeria. Groundw. Sustain. Dev. 20, 100871 https://doi.org/10.1016/j.gsd.2022.100871.

Ozegin, K.O., Ilugbo, S.O., 2024a. A triangulation approach for groundwater potential evaluation using geospatial technology and multi-criteria decision analysis (MCDA) in Edo State, Nigeria. J. Afr. Earth Sci. 209, 105101 https://doi.org/10.1016/j.jafrearsci.2023.105101. (Accessed 6 November 2023).

Ozegin, K.O., Ilugbo, S.O., Adebo, B., 2024b. Spatial evaluation of groundwater vulnerability using the DRASTIC-L model with the analytic hierarchy process (AHP) and GIS approaches in Edo State, Nigeria. Phys. Chem. Earth 134, 103562. https://doi.org/10.1016/j.pce.2024.103562. (Accessed 20 January 2024).

Ozegin K.O., Ilugbo S.O., Alile O.M., Iluore K. 2024c. Integrating in-situ data and spatial decision support systems (SDSS) to identify groundwater potential sites in the Esan plateau, Nigeria. Groundwater for Sustainable Development 26, 101276. doi:10.1016/j.gsd.2024.101276

Palacky, G. J., Ritsema, L. L. and De Jong S. J., 1981. Electromagnetic prospecting for Groundwater in Precambrian terrain in the Republic of Upper Volta. Geophysical Prospecting, 29, Pp. 932-955.